

THE ASTRO OPTICAL RESPONSE MODEL

D. Busonero¹, M. Gai², D. Gardiol², M.G. Lattanzi², D. Loreggia²

¹Università degli Studi di Siena, Italy

²INAF-Osservatorio Astronomico di Torino, Italy

ABSTRACT

We define a numerical description of the signal model for the Gaia astrometric instrument, encoded in the focal plane to sky mapping (FPSM) function, i.e., the transformation between object and image space, and encoded in terms of discrepancy with respect to the geometric optics. We calculate the FPSM for several spectral types, also deriving the chromaticity map.

This model can be extended to take into account dynamic contributions, e.g., attitude or TDI errors. The signal distribution is evaluated to estimate the systematic and random error at the elementary exposure level, and scaled to equivalent final mission performance by means of a simple transformation.

We describe the possible future development of the model into a more detailed realistic representation of the Gaia astrometric measurement.

Key words: Gaia; Astrometry; Instrumentation: miscellaneous; Methods: numerical.

1. INTRODUCTION

The overall description of the Gaia mission goals can be found in other contributions to this meeting (Arenou 2005; Lindegren 2005; Mignard 2005; Perryman 2005; Pace 2005). In this paper we describe the numerical implementation of the detailed signal model used to perform the Gaia performance analysis.

Before entering into the detail of the model we recall the Gaia measurement chain: The measurement concept requires observations along two lines of sight, separated by a large ‘basic angle’ (BA), along the equatorial great circle. So the main astrometric payload is composed of two identical telescopes looking at different lines of sight (LOS) separated by a BA = 99.4°, with a large focal plane (FP) detector (Short 2005): a CCD mosaic of 170 CCDs operated in Time Delay Integration (TDI) mode, 10 CCDs across scan and 17 CCDs along scan direction (2 Sky Mapper [SM], 11 Astro Focal [AF], 4 Broad Band Photometry [BBP]; see Figure 1).

Due to the Gaia scanning mode of operation, the instantaneous star image moves across the detector, in a direction which is mostly co-linear with the CCD columns and y axis of the Gaia reference frame. The TDI allows to achieve a useful integrated image, providing the matching between the continuous satellite motion (resulting in a continuous apparent motion of the image on the focal plane) and the logical pixel array. The instantaneous image is integrated throughout the whole transit over the CCD until it reaches the edge of the device, where the readout process takes place. At this step there is the introduction of the readout noise. Finally, the electric signal is converted to digital form and downloaded to ground.

For each star a window of 6×12 pixels (12×12 for stars brighter than $V = 16$) is selected for read-out. The image is compressed by binning in the across scan (low resolution) direction to minimize telemetry, so that the output data is a one-dimensional signal: $f_n, n = 1, \dots, N$ with $N = 6$ or 12 . The time tag of the exposure is recorded for data processing. Time of observation and position on the sky are linked by the scan law plus optical response. For each transit a target is observed in equal conditions on eleven elementary exposures.

The elementary exposure precision (σ_{exp}) is derived accordingly to centre of gravity (COG):

$$\sigma_{exp}(COG) = \frac{L_{RMS}}{SNR} \quad (1)$$

where L_{RMS} is the RMS width of the effective PSF, and SNR is the signal to noise ratio. The independent composition of the 11 elementary exposures provides the transit-level accuracy. To obtain the final mission accuracy we must take into account data reduction factors for parallax, position and proper motion.

Retaining image quality for detection and read-out requires stable system parameters, known at the mas level; systematic errors associated to system perturbations must also remain below this threshold. At the data reduction level the necessary precision must be at μas level, i.e., three order of magnitude better. The model includes the detailed optical response of the nominal configuration and can easily be applied to perturbed cases. The effect of a realistic optical system is described by the input from ray tracing code (e.g., Code V), as tables of aberration coefficients, used to build a monochromatic PSF

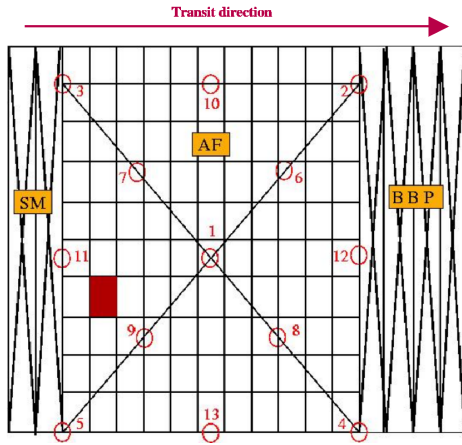


Figure 1. Astro focal plane with the dimension of the effective field of view of the telescope shown by points 1-13.

library over the field, composed to generate the realistic local PSF for different spectral type objects. The signal processing has been developed in the IDL environment.

The instantaneous PSF is processed according to the Gaia operations: CCD response, TDI, windowing, across scan binning. In this context the detector is assumed to be modelled by parameters like Modulation Transfer Function (MTF) and Quantum Efficiency (QE).

In Section 2 below we describe the numerical implementation of the signal model and list the assumptions made to build the model. In Section 3 we provide some detail of the Astro optical model. In Section 4 and 5 we illustrate the various capabilities of our simulator and we present some examples of the FPSM and the chromaticity map. In Section 6 we draw our conclusions.

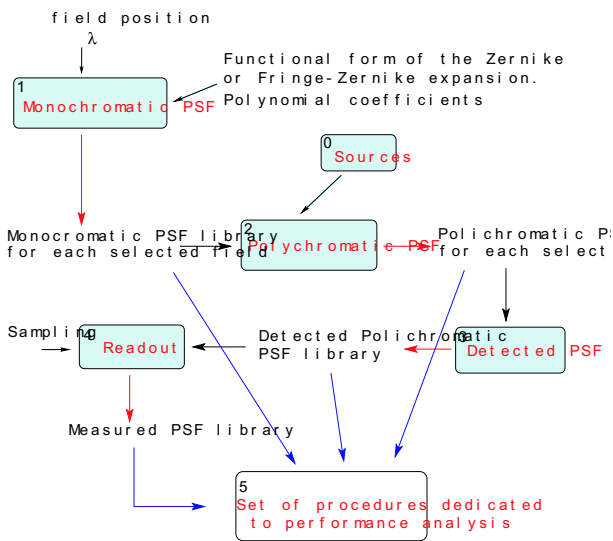


Figure 2. Implementation scheme of the signal model.

2. BUILDING THE SIGNAL MODEL

The numerical implementation of the detailed signal model follows the scheme of Figure 2. The simulator is developed on three different levels:

1. procedures building the monochromatic PSFs library in the wavelength interval [300,1100] nm;
2. procedures for simulation of the polichromatic PSFs and of the measured signal; the output data is a bi-dimensional array;
3. procedures devoted to performance analysis.

Sources: We compute fluxes according to telescope geometry, operations and stellar emission.

Monochromatic PSF: The monochromatic PSF is built in the IDL environment according to diffraction models and local optical response.

Polychromatic PSF: The generation of polychromatic PSFs requires the spectral distribution $S(\lambda)$ for the selected source associated with its effective temperature and scaled according to G magnitude.

The detected PSF: At this step we introduce the ideal pixel response [geometry, MTF]. The finite pixel size increases the L_{RMS} by 18% with respect to the purely optical value.

The measured signal: The selection of the read-out region and across scan binning selection of along scan area and the introduction of the read-out noise provide the transition from the detected PSF to the measured signal. The output is a one-dimensional PSF restricted to the six/twelve central pixels.

Performance analysis: Computation of random noise and systematic errors, e.g., chromaticity.

2.1. Assumptions

The main hypothesis to build the signal model are:

- Source described as black body at the effective temperature T_{eff} for the spectral type;
- the WFE exhibits smooth spatial variation over the focal plane, particularly over a CCD region;
- as a consequence the PSF is locally invariant and has smooth spatial variation over the focal plane (Figure 3);
- the PSF are temporally invariant over short time scale at mas level to preserve the image quality;
- the BA is temporally invariant over short time scale at μ as level;
- the QE and MTF are nearly uniform over a single CCD, so that a representative spectral distribution can be used to compute the photoelectron distribution;

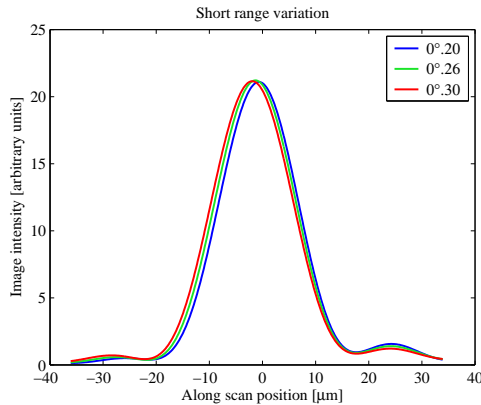


Figure 3. Progressive variation of the image quality over the field; position across scan: $0^\circ.53$; position along scan: $0^\circ.20$, $0^\circ.26$, $0^\circ.30$. PSF at $\lambda = 600$ nm.

- the ideal pixel response can be represented by a rectangular function (100% sensitivity inside the nominal geometric area, 0% outside);
- the real pixel response described by the ideal pixel + MTF + TDI;
- independence of small perturbations with respect to the nominal value for TDI rate and satellite rate, etc;
- given model parameter values.

For most aspects, the signal associated with an elementary exposure on one CCD can be represented by the PSF in the middle of the CCD itself. This assumption is verified in reference cases, and small discrepancies arise only at large angular distance from the optical axis. We consider negligible the perturbation effects at $\leq 1 \mu\text{as}$ level.

3. THE OPTICAL MODEL

We implement in the simulator a realistic optical configuration, representative of the Gaia astrometric payload. It is encoded with the Code V optical ray tracing package and optimized over a field of view (FOV) $0^\circ.66 \times 0^\circ.66$. The monochromatic real PSF I_M is generated according to the diffraction theory as square modulus of the complex amplitude response function, the Fourier Transform of the generalized pupil function (Born & Wolf 1980). The WFE is described by the Zernike expansion provided by the ray tracing code, truncated to 21 terms.

$$I_M(x, y; \lambda) = \left| \iint_A d\zeta d\eta e^{i\Phi(\zeta, \eta)} e^{j \frac{2\pi}{\lambda F} (x\zeta + y\eta)} \right|^2 \quad (2)$$

where $\Phi(\zeta, \eta) = \frac{2\pi}{\lambda} WFE(\zeta, \eta)$ is the pupil function; ζ, η are the pupil coordinates, λ the reference wavelength, F the effective focal length, A the pupil area and (x, y) the focal plane coordinates.

The detected PSF is generated by the contribution of several monochromatic PSFs, weighted according to stellar

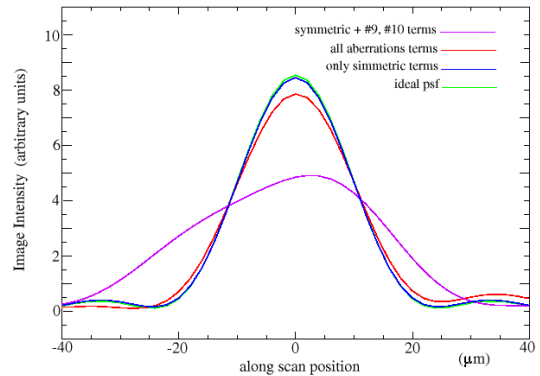


Figure 4. Example of PSF profiles in field position $n^\circ 4$ at $\lambda = 660$ nm with different set of Zernike terms.

spectrum $S(\lambda)$, optical transmission $T(\lambda)$ and quantum efficiency $QE(\lambda)$ and integrated over the spectral range $\Delta\lambda$. The detected energy distribution I_P becomes

$$I_P(x, y) = \int_{\Delta\lambda} d\lambda I_M(x, y; \lambda) \cdot S(\lambda) T(\lambda) QE(\lambda) \quad (3)$$

The aberrations modify the PSF profile over the FP and, consequently, the L_{RMS} value. Moreover, the image quality (and L_{RMS}) changes smoothly over the field of view, giving a variation of the PSF photocentre value over the focal plane. On the other hand, the entrance pupil dimension, the optical transmission $T(\lambda)$ and the quantum efficiency $QE(\lambda)$ of the detector define the signal intensity and the SNR value. Our analysis requires identification of L_{RMS} and SNR over several FOV positions and for several star spectral types to compute the FPSM and the chromaticity map.

In Figure 3 we give a visual representation of the verification of the hypothesis made in Section 2.1 on the local PSF small change. In Figure 4 we show a case of optical performance analysis used to evaluated the different weight of aberration terms on the image quality and consequently on the exposure precision.

3.1. Numerical Implementation

The computation is performed at 13 field positions as showed in Figure 1; in principle it could be performed at any point, but given the assumptions (Section 2.1) the sampling is sufficient.

We generate the monochromatic PSFs according to the CCD spectral response $\Delta\lambda = [300, 1100]$ nm with 10 nm resolution. We use the FFT function in IDL, with fixed sampling step of $2 \mu\text{m}$ on the focal plane, and pupil plane sampling ranging from 74×204 points at $\lambda = 300$ nm to 20×56 points at $\lambda = 1100$ nm. Each PSF is an array of dimension 1024×1024 with a size of 16MB. Due to storage problems the PSFs are saved as a matrix of dimension 257×257 with a size of 1MB, including several Airy lobes.

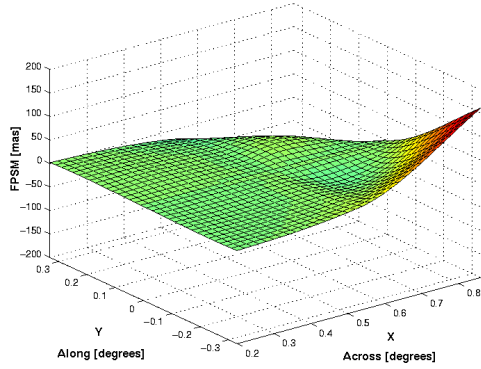


Figure 5. FPSM map for a B3V spectral type.

The total number of the monochromatic PSFs, 81 for each of the 13 selected field positions, gives a total of 1053. For each spectral type and selected field position we generate the polychromatic PSFs, accordingly to Equation 3, and derived the detected and measured signal.

4. FOCAL PLANE TO SKY MAPPING

The Astro optical response is encoded by the Focal Plane to Sky Mapping (FPSM) function. For an ideal telescope there is a linear relation between the angular coordinate on the sky and the linear coordinate on the focal plane, with the proportional factor given by the focal length, F .

In the ideal case the sequence of measurements of a star during its transit on the focal plane generates a linear trajectory due to the fact that the photocentre positions are equally spaced. Instead, a realistic instrument presents a non linear relation due to aberrations. The simplest case is the classical distortion that produces a variable geometric contraction or expansion over the focal plane. Due to the off-axis nature of the Gaia telescope, the displacement from the ideal position is particularly evident at the field corners as shown in Figure 5, where the FPSM map for a B3V spectral type is shown.

Over most of the field, the response is close to the “ideal” telescope, however the effect is large at μas level, becoming relevant at the level of the reduction operation phase. We have to take into account the real star trajectory given by the FPSM map to select the read-out windows following the star during its transit. In addition to the effect already described the blurring of image due to the mismatch between the TDI rate and the scanning speed is also present. For an accurate description of the FPSM, its measurement on science data and its maintenance we refer to Gai (2005).

5. CHROMATICITY

Different spectral type stars, set in the same nominal position, do not have the same estimated position; the same location on the sky is not uniquely mapped on the focal

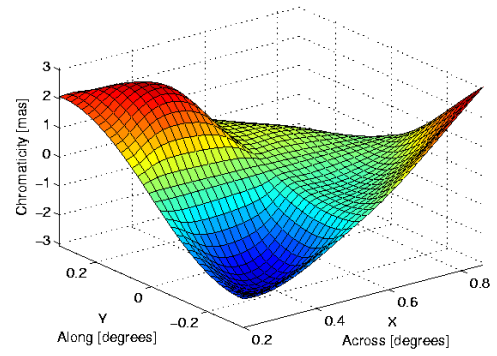


Figure 6. Chromaticity distribution over the astrometric field in the nominal configuration of the Gaia instrument.

plane. We define this colour dependent position variation as chromaticity. It is important to remove this systematic error to preserve the desired mission accuracy.

The chromaticity has been evaluated using the realistic blackbody spectrum associated with the source, either B3V or M8V, deriving the COG and defining the chromaticity as the difference between the B3V and M8V COG. Here only the nominal aberrations are considered, manufacturing and alignment errors are not yet included.

In Figure 6 we show the derived chromaticity map. As we can see, the distribution is symmetric with respect to the y axis due to the symmetry of the optical configuration; the mean chromaticity value is $-0.05 \mu\text{as}$ with RMS value 1.19 mas and a peak value higher than $\pm 2\text{mas}$. At this level, the compensation of opposite errors along the trajectory provides a reduction of the overall chromaticity.

6. CONCLUSIONS

The model described above is a numerical implementation of the Gaia astrometric measurement. It includes a detailed representation of the optical response, detector characteristics and operations. Future development will include additional realistic contributions from optics (manufacturing, integration and alignment); from detector response and geometry and from operation disturbances.

REFERENCES

- Born, M., Wolf, E., 1980, Principles of Optics, Cambridge, University Press, Sixth Ed., Cambridge
- Arenou, F., 2005, ESA SP-576, this volume
- Gai, M., Busonero, D., Gardiol, D., Loreggia, D. 2005, ESA SP-576, this volume
- Lindgren, L., 2005, ESA SP-576, this volume
- Mignard, F., 2005, ESA SP-576, this volume
- Pace, O., 2005, ESA SP-576, this volume
- Perryman, M.A.C., 2005, ESA SP-576, this volume
- Short, A., 2005, ESA SP-576, ESA SP-576, this volume